

# Aerodynamic Sensitivity Theory for Rotary Stability Derivatives

A. C. Limache\* and E. M. Cliff†

Virginia Polytechnic Institute and State University, Blacksburg, Virginia 24061

**A nonlinear boundary-value problem (BVP) is developed to describe the steady compressible flow about a body moving with nonzero angular rates. It is shown that the most general aerodynamically steady motions are characterized by spiral paths. A continuous sensitivity equation method is then applied to develop a linear BVP that characterizes the sensitivity of the flow to changes in angular velocity. The solutions to the sensitivity BVP are used to compute rotary stability derivatives and comparisons are made to some existing methods. The virtue of this approach is that all rotary derivatives can be estimated based on a single solution for the nonlinear flow equations along with three linear sensitivity equations.**

## Nomenclature

|                    |   |
|--------------------|---|
| $C_l, C_d, C_m$    | = lift, drag, and pitching moment coefficients                        |
| $e, E$             | = internal energy, total energy per unit mass                         |
| $\hat{e}$          | = unit vector   |
| $F, H$             | = components of conservative flux vector                              |
| $\bar{F}$          | = steady aerodynamic force function                                   |
| $\mathcal{F}$      | = aerodynamic force functional  |
| $f$                | = body force vector   |
| $M$                | = Mach number   |
| $\dot{M}$          | = pitching moment   |
| $P, T$             | = pressure, temperature   |
| $p, q, r$          | = body roll rate, pitch rate, yaw rate                                |
| $Q$                | = conservative flow variable  |
| $R, R_c$           | = gas constant, radius of circular path                               |
| $\mathcal{R}$      | = general (noninertial) reference frame                               |
| $S_\eta, S_q, S_u$ | = flow sensitivity with respect to $\eta, q$ , and $u$ , respectively |
| $\mathcal{S}$      | = inertial reference frame  |
| $t$                | = time  |
| $u, v, w$          | = flow velocity components  |
| $V, a$             | = speed, acceleration   |
| $W$                | = source terms  |
| $x, y, z$          | = Cartesian coordinates   |
| $x, V, a$          | = vector position, velocity and acceleration, respectively            |
| $\alpha$           | = angle of attack   |
| $\beta$            | = angle of sideslip   |
| $\gamma$           | = ratio of specific heats   |
| $\eta$             | = generic physical parameter  |
| $\rho$             | = air density   |
| $\tau$             | = temporal variable   |
| $\bar{\tau}$       | = shear tensor  |
| $\Omega$           | = inertial body force   |
| $\omega, \omega$   | = angular velocity vector, its magnitude                              |
| <i>Subscripts</i>  |   |
| $c$                | = predetermined point of the aircraft (usually the center of mass)    |

|                            |  |
|----------------------------|--|
| $q, \hat{q}$               | = dimensional and nondimensional pitch rate stability derivatives                      |
| $\mathcal{R}, \mathcal{S}$ | = reference frame ( $\mathcal{R}$ or $\mathcal{S}$ ) in which the variable is measured |
| $\mathcal{R}/\mathcal{S}$  | = origin of reference frame $\mathcal{R}$ as seen from reference frame $\mathcal{S}$   |
| $x, y, z$                  | = Cartesian components   |
| $\alpha$                   | = stability derivatives with respect to angle of attack                                |
| <i>Superscript</i>         |  |
| $\infty$                   | = far-field conditions   |

## Introduction

THE mechanics of atmospheric flight remains an interesting and challenging subject, in part because flight vehicles present a number of complex dynamical components. In the present study computational fluid dynamics (CFD), based on compressible steady flows, is used to model the external aerodynamic forces and moments on rigid aircraft. A continuous sensitivity equation method is used to develop a linear boundary-value problem (BVP) that directly leads to aerodynamic stability derivatives introduced by Bryan (see, for example, the discussion in McRuer, et al<sup>1</sup>) and discussed more recently by Tobak and Schiff.<sup>2</sup> In particular, the focus is on models that describe how the aerodynamic forces and moments depend on angular rates of the rigid aircraft.

The basic idea is that of a sensitivity: loosely, a linear approximation of a nonlinear function. The functions of interest are the maps that associate a flowfield with parameter values. For example, it is shown how one can associate a unique flow solution around an airfoil with each value of its pitch rate. In general, the flowfield is described as the solution of a nonlinear BVP and the parameter(s) could appear in the partial differential equation and/or in the boundary conditions. A model for the flowfield sensitivity is formally derived by implicit differentiation of the nonlinear BVP. The sensitivity method has previously been applied to the calculation of static aerodynamic derivatives<sup>3</sup> and to geometric design analysis for chemically reacting flows.<sup>4</sup> This work extends the approach to the estimation of rotary aerodynamic derivatives.

It is useful to discuss the fluid mechanical models as seen from noninertial reference frames (an inertial reference frame is a reference frame in which Newton's laws hold). This leads to a nonlinear BVP consisting of a nonlinear partial differential equation (PDE) and appropriate boundary conditions. In principle, these equations can be solved by a CFD algorithm, and the associated aerodynamic forces and moments on the body computed by certain weighted surface integrals of the local normal (pressure) and traction forces. It will be seen that the body angular rates appear as coefficients in the nonlinear BVP. The nonlinear BVP is formally differentiated to generate a linear BVP for the flow sensitivity; this flow sensitivity reflects the way the flow variables will change due to a change in

Received 5 August 1999; presented as Paper 99-4919 at the AIAA Atmospheric Flight Mechanics, Portland, OR, 9–11 August 1999; revision received 10 February 2000; accepted for publication 10 February 2000. Copyright © 2000 by A. C. Limache and E. M. Cliff. Published by the American Institute of Aeronautics and Astronautics, Inc., with permission.

\*Graduate Assistant, Aerospace and Ocean Engineering Department and the Interdisciplinary Center for Applied Mathematics; alimache@icam.vt.edu.

†Reynolds Metals Professor, Aerospace and Ocean Engineering Department and the Interdisciplinary Center for Applied Mathematics; cliff@icam.vt.edu. Associate Fellow AIAA.

the physical parameter. These ideas are applied to determine rotary stability derivatives by choosing the parameter to be the pitch rate. These rotary stability derivatives are computed by a weighted integral over the body surface of the pressure sensitivity.

### Preliminary Remarks

From a flight mechanics point of view, one is interested in a description of the aerodynamic forces acting on a flight vehicle. A mathematical model for these forces can be developed in terms of a nonlinear PDE with boundary conditions for the PDE that include appropriate conditions at the fluid/vehicle interface. With this structure in mind a generic aerodynamic force is expressed as

$$F(t) = \mathcal{F}(V_c(\tau), \alpha(\tau), \beta(\tau), p(\tau), q(\tau), r(\tau), t) \quad (1)$$

where  $\tau$  is a temporal parameter going from  $-\infty$  to time  $t$ . This functional form indicates that the aerodynamic forces depend on the history of the dynamic variables: speed  $V_c$ , angle of attack  $\alpha$ , angle of sideslip  $\beta$ , and the angular rates  $p, q$ , and  $r$  defining the particular trajectory of the aircraft. The idea that the aerodynamic forces are described by a functional and depend on the past history of the motion was noted by von Kármán and Burgers.<sup>5</sup> The classic works of Theodorsen<sup>6</sup> and Jones<sup>7</sup> provided approximate representations for this functional in the case of incompressible flow about a thin airfoil. More recently, Herdman and Tur<sup>8</sup> have rigorously studied a representation based on neutral functional differential equations.

It is certainly possible, within some limitations, to generate numerically time-accurate CFD solutions to determine the aerodynamic forces acting on an aircraft. This has been demonstrated<sup>9</sup> for flow models based on vortex-lattice methods.

More commonly, CFD approaches are restricted to the special case wherein the aircraft is in steady, rectilinear, wings-level flight, that is, when the aircraft is flying at constant values of  $V_c$ ,  $\alpha$ , and  $\beta$  and with zero angular rates. In this case (assuming a steady flow exists) the aerodynamic forces are constant and Eq. (1) reduces to

$$F = \bar{F}(V_c, \alpha, \beta, 0, 0, 0) \quad (2)$$

Note that the first six arguments of the functional  $\mathcal{F}$  in Eq. (1) are real-valued functions, whereas the corresponding arguments of  $\bar{F}$  in Eq. (2) are real numbers.

In the present study, the class of steady motions is generalized to include motions with nonzero angular rates. This requires extending the standard CFD formulation to general noninertial reference frames.

### Fluid Motions in Noninertial Frames

In subsequent discussions it is assumed that the reader is familiar with relations among the various (relative) positions, velocities, and accelerations. This material may be found in standard references, such as those of Etkin<sup>10</sup> or Miele.<sup>11</sup>

Consider two observers, one located at the origin  $O_S$  of a coordinate system defined in an inertial reference frame denoted by  $\mathcal{S}$  and the other observer located at the origin  $O_R$  of a coordinate system defined in a general reference frame denoted by  $\mathcal{R}$ . At a given time  $t$ , the observer in the general reference frame  $\mathcal{R}$  will be located at a position  $\mathbf{x}_{R/S}(t)$  with respect to  $\mathcal{S}$  and will be moving with a velocity

$$V_{R/S}(t) = \frac{d\mathbf{x}_{R/S}}{dt} \Big|_{\mathcal{S}}$$

and an acceleration

$$\mathbf{a}_{R/S}(t) = \frac{dV_{R/S}}{dt} \Big|_{\mathcal{S}}$$

with respect to  $\mathcal{S}$ . Furthermore, at the same time, the frame  $\mathcal{R}$  may be also rotating with instantaneous angular rate  $\boldsymbol{\omega}(t)$  with respect to the inertial frame  $\mathcal{S}$ .

The equations that govern the fluid motion as seen from the observer in the noninertial frame  $\mathcal{R}$  are a generalization of the formulation given by Hirsch<sup>12</sup> (see page 16 and those that follow).

Equation of conservation of mass or continuity equation

$$\frac{\partial \rho}{\partial t} + \nabla \cdot (\rho \mathbf{V}_R) = 0 \quad (3)$$

Equation of conservation of momentum

$$\frac{\partial \rho \mathbf{V}_R}{\partial t} + \nabla \cdot [\rho \mathbf{V}_R \otimes \mathbf{V}_R + P \vec{I} - \vec{\tau}] = \rho [\mathbf{f} + \boldsymbol{\Omega} - 2\boldsymbol{\omega} \times \mathbf{V}_R] \quad (4)$$

Equation of conservation of energy

$$\frac{\partial \rho E}{\partial t} + \nabla \cdot [(\rho E + P) \mathbf{V}_R - \vec{\tau} \cdot \mathbf{V}_R - k_T \nabla T] = \rho [\mathbf{f} + \boldsymbol{\Omega} \cdot \mathbf{V}_R + q_v] \quad (5)$$

In Eqs. (3–5), the variables are expressed in a Eulerian (local) way as seen from the noninertial rotating frame  $\mathcal{R}$ . In this sense,  $\mathbf{V}_R$  is the local velocity of the flow as seen from the rotating reference frame, and  $E$  is the total energy (per unit of mass) as seen from the rotating frame:

$$E = e + \frac{1}{2} \mathbf{V}_R \cdot \mathbf{V}_R$$

Also,  $\mathbf{f}$  is net body force and  $\boldsymbol{\Omega}$  is the pseudoforce vector

$$\boldsymbol{\Omega} = -\boldsymbol{\omega} \times (\boldsymbol{\omega} \times \mathbf{x}_R) - \frac{d\boldsymbol{\omega}}{dt} \times \mathbf{x}_R - \mathbf{a}_{R/S}$$

that contains the effect of the noninertial motion (except for the Coriolis term  $-2\boldsymbol{\omega} \times \mathbf{V}_R$ ).  $\mathbf{V} \otimes \mathbf{V}$  is a second order tensor defined in terms of its components in Cartesian coordinates as  $[\mathbf{V} \otimes \mathbf{V}]_{ij} \equiv [\mathbf{V}]_i [\mathbf{V}]_j$ , where  $[\mathbf{V}]_i$  is the  $i$ th component of the velocity vector.  $\vec{I}$  is the identity tensor and  $\vec{\tau}$  is the stress tensor; each of these is a second-order tensor.

In the following, the subindex  $\mathcal{R}$  is dropped from the velocity  $\mathbf{V}_R$ , the position vector  $\mathbf{x}_R$ , and the unit vectors  $\hat{e}_x, \hat{e}_y$ , and  $\hat{e}_z$  because unless otherwise specified all quantities are referred to the noninertial frame  $\mathcal{R}$ . The vectors  $\mathbf{x}_R, \mathbf{V}_R, \boldsymbol{\omega}$ , and  $\boldsymbol{\Omega}$ , when resolved in terms of their components in the noninertial frame  $\mathcal{R}$ , will be written simply as

$$\begin{aligned} \mathbf{x} &= x \hat{e}_x + y \hat{e}_y + z \hat{e}_z, & \mathbf{V} &= u \hat{e}_x + v \hat{e}_y + w \hat{e}_z \\ \boldsymbol{\omega} &= p \hat{e}_x + q \hat{e}_y + r \hat{e}_z, & \boldsymbol{\Omega} &= \Omega_x \hat{e}_x + \Omega_y \hat{e}_y + \Omega_z \hat{e}_z \end{aligned}$$

respectively.

### Conservative Form of Two-Dimensional Flows in Noninertial Frames

For the case of a two-dimensional flow in the  $x, z$  plane,  $\boldsymbol{\omega}$  is reduced to  $\boldsymbol{\omega} = q \hat{e}_y$ . Additionally, assuming an inviscid, nonconducting fluid, the flow equations (3–5) can be written in the Cartesian coordinate system  $x, y, z$  of the noninertial reference frame  $\mathcal{R}$  in the compact form

$$\frac{\partial Q}{\partial t} + \frac{\partial F}{\partial x} + \frac{\partial H}{\partial z} = W$$

where

$$Q = \begin{bmatrix} Q_1 \\ Q_2 \\ Q_3 \\ Q_4 \end{bmatrix} = \begin{bmatrix} \rho \\ \rho u \\ \rho w \\ \rho E \end{bmatrix} \quad (6)$$

is the vector of conserved quantities,

$$F = \begin{bmatrix} \rho u \\ \rho uu + P \\ \rho uw \\ u(\rho E + P) \end{bmatrix}, \quad H = \begin{bmatrix} \rho w \\ \rho uw \\ \rho ww + P \\ w(\rho E + P) \end{bmatrix}$$

are the components of the inviscid fluxes, and  $W$ , under the assumption of no external forces, is given by

$$W = \begin{bmatrix} 0 \\ \rho\Omega_x - 2\rho q w \\ \rho\Omega_z + 2\rho q u \\ \rho\Omega_x u + \rho\Omega_z w \end{bmatrix} \quad (7)$$

It can be seen that the form of the flow equations in the noninertial frame is identical to the form in an inertial reference frame except for the additional source term  $W$ . By the use of this fact, a conservative formulation is developed in exactly the same way as in CFD for flows in inertial reference frames. In particular, observe that the fluxes  $F$  and  $H$  can be written in conservative form as

$$F = \begin{bmatrix} Q_2 \\ \frac{Q_2^2}{Q_1} + (\gamma - 1) \left( Q_4 - \frac{Q_2^2 + Q_3^2}{2Q_1} \right) \\ \frac{Q_2 Q_3}{Q_1} \\ \frac{Q_2}{Q_1} \left( \gamma Q_4 - \frac{(\gamma - 1)(Q_2^2 + Q_3^2)}{2Q_1} \right) \end{bmatrix} \quad (8)$$

$$H = \begin{bmatrix} Q_3 \\ \frac{Q_3 Q_2}{Q_1} \\ \frac{Q_3^2}{Q_1} + (\gamma - 1) \left( Q_4 - \frac{Q_2^2 + Q_3^2}{2Q_1} \right) \\ \frac{Q_3}{Q_1} \left( \gamma Q_4 - \frac{(\gamma - 1)(Q_2^2 + Q_3^2)}{2Q_1} \right) \end{bmatrix} \quad (9)$$

A similar fact is true for the pressure  $P$ , that is, for a calorically perfect gas one can write

$$P = (\gamma - 1) Q_1 \left( Q_4 / Q_1 - \frac{1}{2} [(Q_2 / Q_1)^2 + (Q_3 / Q_1)^2] \right)$$

These expressions are identical to the relations of the thermodynamic variables and fluxes in terms of conservative variables in inertial frames. The difference lies in the source term  $W$ . By the use of Eqs. (6) and (7), the source term can also be expressed completely in terms of the conservative variables and the variables describing the motion of the reference frame, namely,

$$W = \begin{bmatrix} 0 \\ Q_1 \Omega_x - 2q Q_3 \\ Q_1 \Omega_z + 2q Q_2 \\ \Omega_x Q_2 + \Omega_z Q_3 \end{bmatrix} \quad (10)$$

### Boundary Conditions

The boundary conditions along solid walls are different for Navier-Stokes (viscous) flows and for Euler flows. In the former case, the velocity of the flow vanishes at solid walls, whereas in the case of Euler flows, there is no flow through the wall, that is,

$$\mathbf{V} \cdot \hat{\mathbf{n}} = 0$$

In general, the boundary conditions applied at the far-field boundary are the same for Navier-Stokes and Euler flows. Many of the physical boundary conditions in external flows are of the type of matching with given far-field conditions  $Q^\infty$ , that is,

$$\lim_{\|\mathbf{x}\| \rightarrow \infty} Q_S = Q^\infty$$

where the subscript  $S$  indicates that the values of the flow variables at the far field are defined as seen from the inertial frame  $S$ . However, because certain thermodynamic variables, density  $\rho$ , pressure

$P$ , temperature  $T$ , entropy  $s$ , internal energy  $e$ , and the speed of sound  $a$ , are scalar quantities, they are independent of the reference frame. [Note that the speed of sound  $a = \sqrt{(\partial P / \partial \rho)_s}$  is also a thermodynamic property of the state of fluid. For a thermally perfect gas,  $a = \sqrt{(\gamma RT)}$ .] This implies that

$$\lim_{\|\mathbf{x}\| \rightarrow \infty} f(\mathbf{x}) = f^\infty$$

where  $f$  is replaced by any of the symbols  $\{\rho, P, T, a, e\}$ .

The only variable that requires special care is the flow velocity that depends on the reference frame because it is a vector quantity. The velocity of interest is as seen from the noninertial reference frame  $\mathcal{R}$ :

$$\lim_{\|\mathbf{x}\| \rightarrow \infty} \mathbf{V}(\mathbf{x}) = \lim_{\|\mathbf{x}\| \rightarrow \infty} \mathbf{V}_S(\mathbf{x}) - \mathbf{V}_{\mathcal{R}/S} - \boldsymbol{\omega} \times \mathbf{x}$$

In the case where the unperturbed air is at rest in the inertial frame  $S$ , this simplifies to

$$\lim_{\|\mathbf{x}\| \rightarrow \infty} \mathbf{V}(\mathbf{x}) = -\mathbf{V}_{\mathcal{R}/S} - \lim_{\|\mathbf{x}\| \rightarrow \infty} \boldsymbol{\omega} \times \mathbf{x}$$

which written in components reads

$$\lim_{\|\mathbf{x}\| \rightarrow \infty} \begin{bmatrix} u \\ v \\ w \end{bmatrix} = \lim_{\|\mathbf{x}\| \rightarrow \infty} \begin{bmatrix} -u_{\mathcal{R}/S} - (qz - ry) \\ -v_{\mathcal{R}/S} - (rx - pz) \\ -w_{\mathcal{R}/S} - (py - qx) \end{bmatrix} \quad (11)$$

From these one can deduce the far-field conditions for the conserved variables, which are applied computationally at large  $\|\mathbf{x}\|$ , for example,  $\|\mathbf{x}\|$  equals 20 chord lengths.

### Kinematics of Steady Motion

The property of steadiness in a fluid motion depends on a number of issues including the choice of observer. Commonly, the vehicle is translating at a constant velocity without rotating, and one uses a Galilean transformation to view the fluid motion from the pilot's point of view; in this setting, the vehicle is in a steady motion. In the following this result is generalized to include rotational motion.

Consider the vector  $\mathbf{V}_c$  that describes the translational velocity of a specified point on the aircraft (usually the center of mass) with respect to a fixed observer in the inertial reference frame  $S$ , where the undisturbed air is assumed to be at rest. Note that the quantities  $V_c$ ,  $\alpha$ , and  $\beta$  are scalars so that their rates of change are independent of the reference frame. For vector quantities, such as  $\mathbf{V}_c$ , the rates of change in two reference frames are related by the standard Eulerian formula

$$\frac{d\mathbf{V}_c}{dt} \Big|_S = \frac{d\mathbf{V}_c}{dt} \Big|_{\mathcal{R}} + \boldsymbol{\omega} \times \mathbf{V}_c \quad (12)$$

where  $\boldsymbol{\omega}$  is the angular velocity of frame  $\mathcal{R}$  with respect to frame  $S$ .

For an aerodynamically steady motion the aerodynamic angles  $\alpha$  and  $\beta$  must remain constant and this implies 1) that the orientation of any body frame is fixed with respect to the wind-frame and 2) that the velocity of the body frame with respect to the inertial frame is a fixed vector in the body frame.

From the first, one deduces that the body frame and the wind frame have the same angular velocity with respect to the inertial frame. Furthermore, in a steady motion, the components of the angular velocity are constant, and this implies that  $d\boldsymbol{\omega}/dt = 0$ .

The second conclusion means that

$$\frac{d\mathbf{V}_c}{dt} \Big|_{\mathcal{R}} = \mathbf{0}$$

and this, combined with Eq. (12), leads to a simple system of linear, constant-coefficient, ordinary differential equations for the components of  $\mathbf{V}_c$  in the inertial frame:

$$\frac{d\mathbf{V}_c}{dt} \Big|_{\mathcal{S}} = \omega \times \mathbf{V}_c \quad (13)$$

System (13) can be integrated to yield

$$\begin{bmatrix} u_{cS}(t) \\ v_{cS}(t) \\ w_{cS}(t) \end{bmatrix} = \left( \mathbf{V}_{c0} \cdot \frac{\omega}{\omega} \right) \frac{\omega}{\omega} + \left[ \mathbf{V}_{c0} - \left( \mathbf{V}_{c0} \cdot \frac{\omega}{\omega} \right) \frac{\omega}{\omega} \right] \cos(\omega t) + \left( \frac{\omega}{\omega} \times \mathbf{V}_{c0} \right) \sin(\omega t) \quad (14)$$

A second integration gives the inertial-frame position components as

$$\begin{bmatrix} x_{cS}(t) \\ y_{cS}(t) \\ z_{cS}(t) \end{bmatrix} = \begin{bmatrix} x_{c0} \\ y_{c0} \\ z_{c0} \end{bmatrix} + \left( \mathbf{V}_{c0} \cdot \frac{\omega}{\omega} \right) \left( \frac{\omega}{\omega} \right) t + \left[ \mathbf{V}_{c0} - \left( \mathbf{V}_{c0} \cdot \frac{\omega}{\omega} \right) \frac{\omega}{\omega} \right] \frac{\sin(\omega t)}{\omega} - \left( \frac{\omega}{\omega} \times \mathbf{V}_{c0} \right) \frac{\cos(\omega t)}{\omega} \quad (15)$$

Equations (14) and (15) are a parametric description of a spiral. Note that Eq. (14) includes a constant component along the direction  $\mathbf{e}_\omega = \omega/\omega$  and a harmonic part. The constant vector multiplying  $\cos(\omega t)$  in Eq. (14) is the orthogonal complement of the constant part, whereas the constant vector multiplying  $\sin(\omega t)$  is orthogonal to the plane spanned by  $\{\mathbf{V}_{c0}, \mathbf{e}_\omega\}$ . The magnitude of the vectors in the harmonic part are, in fact, equal. This means that such spiral motions are the most general motion of an aircraft for which a steady description is possible. For a related discussion, see the classical book by von Mises.<sup>13</sup>

## Two-Dimensional Steady Motions

As an example of the general formulation just described, attention is restricted to the forces on an airfoil in inviscid flow. In the usual case the airfoil is in simple rectilinear motion with zero angular rates. Obviously, the flow will be two dimensional, and a standard CFD code for steady flow can be used to determine the aerodynamic forces [cf. Eq. (2)].

$$\mathbf{F} = \bar{\mathbf{F}}(\mathbf{V}_c, \alpha, 0, 0, 0, 0) \quad (16)$$

In particular, the lift  $C_l(M, \alpha)$ , drag  $C_d(M, \alpha)$ , and pitching moment  $C_m(M, \alpha)$  coefficients can be calculated for different values of speed (or Mach number  $M$ ) and angle of attack. Examples of these calculation using CFD are shown in Figs. 1 and 2 for a NACA 0012 airfoil. The general streamline pattern and the pressure contours are shown for a Mach number  $M = 0.1$  (Fig. 1) and for a Mach number  $M = 0.8$  (Fig. 2) at angle of attack  $\alpha = 0$ . The CFD program that was used here is referred to as the Class Code; it is based on a finite volume formulation on unstructured grids and was provided by Kyle Anderson from NASA Langley Research Center.

Observe that with this code one could determine the stability derivatives ( $C_{l_\kappa}, C_{d_\kappa}, C_{m_\kappa}$ ,  $\kappa \in \{M, \alpha\}$ ) of the aerodynamic forces and moments with respect to the angle of attack  $\alpha$  and flight Mach number  $M$  (or speed  $\mathbf{V}_c$ ) by finite differences. For example,  $C_{l_\alpha}$  could be calculated by using two flow solutions so that

$$C_{l_\alpha} = [C_l(M, \alpha + \Delta\alpha) - C_l(M, \alpha)]/\Delta\alpha$$

Alternatively, such static aerodynamic stability derivatives can be evaluated by a sensitivity equation approach, as done by Godfrey and Cliff.<sup>3</sup> The sensitivity approach is computationally cheaper in the sense that it will require only one nonlinear flow solution plus solving a linear PDE, instead of the two nonlinear solutions required in finite differences.

On the other hand, because the Class Code and the sensitivity formulation developed by Godfrey and Cliff<sup>3</sup> are both based in an

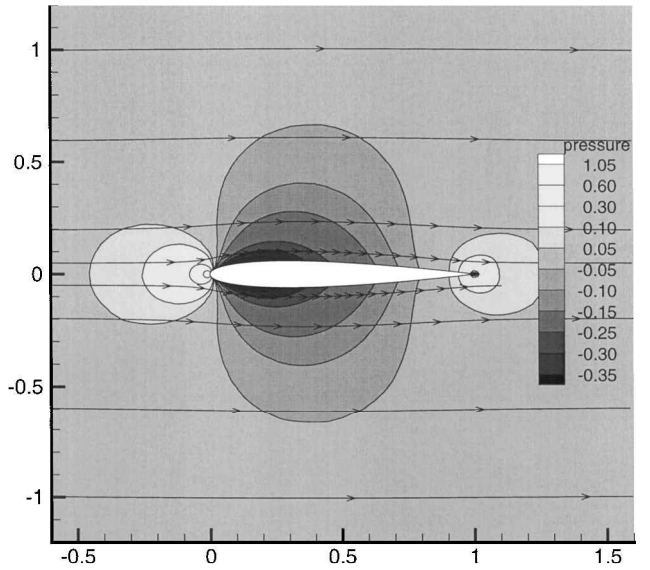


Fig. 1 Pressure contours and streamlines for flow around a NACA 0012 airfoil at  $M = 0.1$  and  $\alpha = 0.0$  deg.

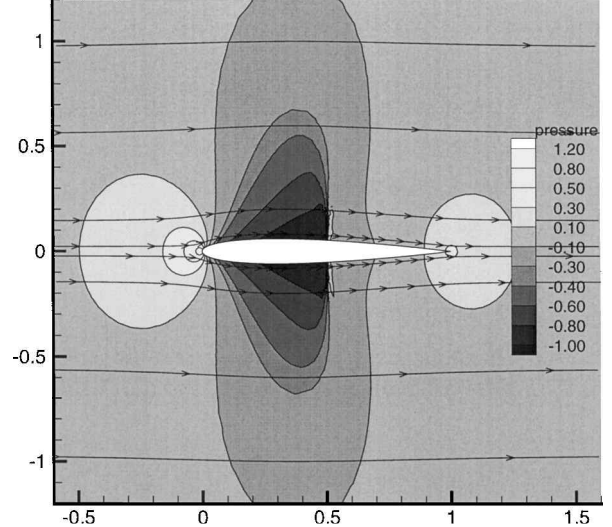


Fig. 2 Pressure contours and streamlines for flow around a NACA 0012 airfoil at  $M = 0.8$  and  $\alpha = 0.0$  deg.

inertial formulation, where the airfoil is not allowed to pitch, neither can be used to evaluate the pitch-rate derivatives  $C_{l_q}$ ,  $C_{d_q}$ , and  $C_{m_q}$ . To estimate such terms, it is necessary to account for the possibility of nonzero pitch rates  $q$  by finding the appropriate steady motion of the airfoil in a planar motion but with nonzero pitch rates.

Note that the general steady motion discussed in the preceding section can be restricted to the case where  $\omega$  and  $\mathbf{V}_0$  are orthogonal. In this case, Eq. (15) reduces to (modulo the initial position)

$$\begin{bmatrix} x_{cS}(t) \\ y_{cS}(t) \\ z_{cS}(t) \end{bmatrix} = \left( \frac{\mathbf{V}_{c0}}{\omega} \right) \sin(\omega t) - \left( \frac{\omega}{\omega} \times \frac{\mathbf{V}_{c0}}{\omega} \right) \cos(\omega t)$$

Moreover, the constant vector multiplying  $\sin(\omega t)$  has the same magnitude as that multiplying  $\cos(\omega t)$  and is orthogonal to it. It is clear that the motion is planar, and in fact it follows a circular path, as shown for the aircraft in Fig. 3. In this case the motion has the following features:

- 1) The radius of the circular path  $R_c$  is related to the pitch rate and the speed of the aircraft through  $V_c = R_c q$ .
- 2) The aircraft experiences a centripetal acceleration

$$a_c = V_c^2 / R_c$$

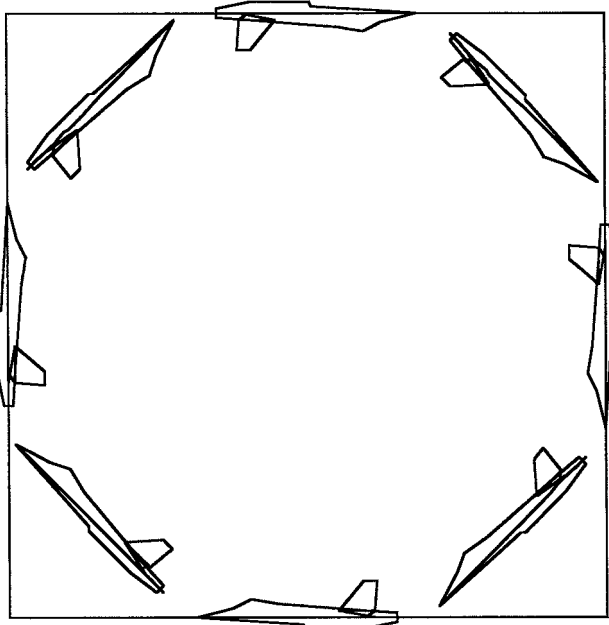


Fig. 3 Aircraft flying in a circular path with constant pitch rate  $q$  and constant angle of attack  $\alpha$ .

which is normal to the velocity vector. This guarantees that the aircraft is not changing its speed.

3) From the pilot's view the flow motion is steady.

However, the use of the standard (inertial) CFD equations is not valid. The two-dimensional CFD formulation in general noninertial reference frames, as described earlier, is needed. This generalized two-dimensional CFD formulation is also used to develop a sensitivity formulation for the calculation of rotary stability derivatives. The case of planar motion that only can be applied to calculate stability derivatives with respect to a pitch rate  $q$  is considered. The ideas presented can be extended to the three-dimensional case to calculate the whole set of rotary derivatives, that is, derivatives in roll  $p$ , pitch  $q$ , and yaw  $r$ .

### Flow Sensitivity Equations

In this section the equations for the flow sensitivities with respect to a general parameter  $\eta$  is described. The parameter could modify the far-field conditions, the flow equations, or both. For simplicity it is assumed that the parameter does not modify the shape of the aircraft or any other boundary geometry, and attention is restricted to two-dimensional Euler flows, that is, the fluid is inviscid and nonheat conducting.

Because the state of a two-dimensional Euler flow is completely defined in terms of the four conserved quantities (6), then the sensitivities  $S_\eta$  of the conserved quantities  $Q$  with respect to the parameter  $\eta$  will be a vector with four components:

$$\begin{bmatrix} S_{\eta 1} \\ S_{\eta 2} \\ S_{\eta 3} \\ S_{\eta 4} \end{bmatrix} = S_\eta = \frac{\partial}{\partial \eta} Q(\mathbf{x}, t; \eta) = \begin{bmatrix} \frac{\partial Q_1(\mathbf{x}, t; \eta)}{\partial \eta} \\ \frac{\partial Q_2(\mathbf{x}, t; \eta)}{\partial \eta} \\ \frac{\partial Q_3(\mathbf{x}, t; \eta)}{\partial \eta} \\ \frac{\partial Q_4(\mathbf{x}, t; \eta)}{\partial \eta} \end{bmatrix} \quad (17)$$

From the flow equations it is possible to determine the differential equation satisfied by the sensitivity vector  $S_\eta$ .

Observe that if the sensitivities of the conserved variables are known, then the sensitivities of any of the primitive variables

$\{\rho, P, e, T, u, w\}$  can be calculated. For example, the sensitivity  $S_u$  of the  $x$  component of the velocity can be determined from

$$S_u = \frac{\partial u}{\partial \eta} = \frac{\partial Q_2/Q_1}{\partial \eta} = -\frac{Q_2}{Q_1^2} \frac{\partial Q_1}{\partial \eta} + \frac{1}{Q_1} \frac{\partial Q_2}{\partial \eta}$$

Note that the flux functions  $F$  and  $H$  depend explicitly on  $Q$  only. The dependence on  $x$ ,  $t$ , and  $\eta$  is through the chain rule. The source-term  $W$  may depend on  $\eta$  explicitly, as well as implicitly through  $Q$ . Taking the derivative of the flow equation with respect to the parameter  $\eta$ , one finds

$$\frac{\partial}{\partial \eta} \frac{\partial}{\partial t} Q + \frac{\partial}{\partial \eta} \frac{\partial}{\partial x} F(Q) + \frac{\partial}{\partial \eta} \frac{\partial}{\partial z} H(Q) = \frac{\partial}{\partial \eta} W(Q; \eta)$$

Because the spatial coordinates  $x$  and the time  $t$  are independent of the  $\eta$  parameter, and assuming certain smoothness, the order of differentiation can be interchanged

$$\frac{\partial}{\partial t} \frac{\partial}{\partial \eta} Q + \frac{\partial}{\partial x} \frac{\partial}{\partial \eta} F(Q) + \frac{\partial}{\partial z} \frac{\partial}{\partial \eta} H(Q) = \frac{\partial}{\partial \eta} W(Q; \eta) \quad (18)$$

Differentiating flux expression (8) with respect to  $\eta$  by using the chain rule leads to

$$\frac{\partial}{\partial \eta} F[Q(\mathbf{x}, t; \eta)] = \nabla_Q F \cdot \frac{\partial Q}{\partial \eta}(\mathbf{x}, t; \eta)$$

where  $\nabla_Q F$  is the Jacobian of  $F$  with respect to the conserved quantities  $Q$ . Similar expressions for the conservative flux  $H$  can be derived, and using definition (17), Eq. (18) is rewritten as

$$\frac{\partial S_\eta}{\partial t} + \frac{\partial}{\partial x} [\nabla_Q F \cdot S_\eta] + \frac{\partial}{\partial z} [\nabla_Q H \cdot S_\eta] = \frac{\partial}{\partial \eta} W(Q; \eta) \quad (19)$$

For the term  $(\partial/\partial \eta)W(Q; \eta)$ , Eq. (10) is formally differentiated:

$$\frac{\partial}{\partial \eta} W = \begin{bmatrix} 0 \\ \frac{\partial Q_1}{\partial \eta} \Omega_x - 2q \frac{\partial Q_3}{\partial \eta} \\ \frac{\partial Q_1}{\partial \eta} \Omega_z + 2q \frac{\partial Q_2}{\partial \eta} \\ \Omega_x \frac{\partial Q_2}{\partial \eta} + \Omega_z \frac{\partial Q_3}{\partial \eta} \end{bmatrix} + \begin{bmatrix} 0 \\ Q_1 \frac{\partial \Omega_x}{\partial \eta} - 2 \frac{\partial q}{\partial \eta} Q_3 \\ Q_1 \frac{\partial \Omega_z}{\partial \eta} + 2 \frac{\partial q}{\partial \eta} Q_2 \\ \frac{\partial \Omega_x}{\partial \eta} Q_2 + \frac{\partial \Omega_z}{\partial \eta} Q_3 \end{bmatrix}$$

As a consequence,

$$\frac{\partial}{\partial \eta} W[Q(\mathbf{x}, t; \eta); \eta] = W_A[Q(\mathbf{x}, t; \eta); \eta] \cdot S_\eta + W_B[Q(\mathbf{x}, t; \eta); \eta] \quad (20)$$

where

$$W_A(Q; \eta) = \begin{bmatrix} 0 & 0 & 0 & 0 \\ \Omega_x & 0 & -2q & 0 \\ \Omega_z & 2q & 0 & 0 \\ 0 & \Omega_x & \Omega_z & 0 \end{bmatrix} \quad (21)$$

and

$$W_B(Q; \eta) = \begin{bmatrix} 0 \\ Q_1 \frac{\partial \Omega_x}{\partial \eta} - 2 \frac{\partial q}{\partial \eta} Q_3 \\ Q_1 \frac{\partial \Omega_z}{\partial \eta} + 2 \frac{\partial q}{\partial \eta} Q_2 \\ \frac{\partial \Omega_x}{\partial \eta} Q_2 + \frac{\partial \Omega_z}{\partial \eta} Q_3 \end{bmatrix} \quad (22)$$

With the substitution of Eq. (20) into Eq. (19), it follows that the sensitivities  $S_\eta$  satisfy

$$\frac{\partial S_\eta}{\partial t} + \frac{\partial}{\partial x} [\nabla_Q F \cdot S_\eta] + \frac{\partial}{\partial z} [\nabla_Q H \cdot S_\eta] = W_A \cdot S_\eta + W_B \quad (23)$$

If this is solved with the appropriate boundary conditions, the flow sensitivity  $S_\eta$  can be determined. Whereas equation (23) may seem complicated, it is, in fact, a linear PDE. Observe that the Jacobians  $\nabla_Q F$  and  $\nabla_Q H$  are known functions of the flow solution and independent of the sensitivities, as are the matrices  $W_A$  and  $W_B$ .

### Rotary Stability Derivatives

As an example of the use of the sensitivity equation method in flight mechanics, the flow sensitivity with respect to the pitch rate is determined. From Eq. (23) the sensitivity vector for the pitch rate  $q$  satisfies the linear PDE,

$$\frac{\partial S_q}{\partial t} + \frac{\partial}{\partial x} [\nabla_Q F \cdot S_q] + \frac{\partial}{\partial z} [\nabla_Q H \cdot S_q] = W_A \cdot S_q + W_B \quad (24)$$

where  $W_A$  is given by Eq. (21) and  $W_B(Q; q)$  from Eq. (22) is given by

$$W_B(Q; q) = \begin{bmatrix} 0 \\ Q_1 \frac{\partial \Omega_x}{\partial q} - 2Q_3 \\ Q_1 \frac{\partial \Omega_z}{\partial q} + 2Q_2 \\ \frac{\partial \Omega_x}{\partial q} Q_2 + \frac{\partial \Omega_z}{\partial q} Q_3 \end{bmatrix} \quad (25)$$

The general vector relationship for  $\Omega$  is

$$\Omega \equiv -\omega \times (\omega \times x_R) - \frac{d\omega}{dt} \times x_R - \alpha_{R/S}$$

and for the two-dimensional case treated here, this reduces to

$$\begin{bmatrix} \Omega_x \\ \Omega_z \end{bmatrix} = \begin{bmatrix} q^2 x - q w_c \\ q^2 z + q u_c \end{bmatrix}$$

Thus, expression (25) becomes

$$W_B(Q; q) = \begin{bmatrix} 0 \\ Q_1(2qx - w_c) - 2Q_3 \\ Q_1(2qz + u_c) + 2Q_2 \\ (2qx - w_c)Q_2 + (2qz + u_c)Q_3 \end{bmatrix} \quad (26)$$

Note that, when calculating the pitch-rate derivatives in the case of steady, straight, and level flight ( $p = q = r = 0$ ), the term  $W_A$  vanishes and  $W_B$  in Eq. (26) reduces to

$$W_B(Q; 0) = \begin{bmatrix} 0 \\ -Q_1 w_c - 2Q_3 \\ Q_1 u_c + 2Q_2 \\ -w_c Q_2 + u_c Q_3 \end{bmatrix}$$

Once the linear problem posed by Eq. (24) is solved, the pressure sensitivity  $\partial P / \partial q$  is available at any point in the flowfield. In the case of Euler flows, this is sufficient to calculate the sensitivities of each of the aerodynamic forces and moments with respect to the pitch rate. For example, the pitching moment is computed by the following weighted integral of the pressure  $P$  around the body surface  $\Sigma$ :

$$\hat{M} = \int_{\Sigma} [x \times -P \hat{n}]_y \, d\sigma$$

It follows then that the sensitivity of the pitching moment with respect to the pitch rate ( $\partial \hat{M} / \partial q$ ) is given by

$$\frac{\partial \hat{M}}{\partial q} = - \int_{\Sigma} \left[ \frac{\partial P}{\partial q} \right] [x \times \hat{n}]_y \, d\sigma \quad (27)$$

Observe that all of the procedures used to compute the aerodynamic forces can be used to compute their sensitivities by simply replacing the pressure by the pressure sensitivity.

### Numerical Results: Pitch-Rate Sensitivity

A solution procedure for the two-dimensional sensitivity equation (24) was implemented using a finite volume formulation. The NISFLOW code can calculate sensitivities with respect to the angle of attack  $\alpha$ , the Mach number  $M$ , and the pitch rate  $q$ . The same unstructured grid that was used for the flow solution was used to compute the flow sensitivities. Note that, although it may be convenient to solve the sensitivity equation using the same scheme and discretization as for the nonlinear flow, it is not necessary to do so. Indeed, when using adaptive grid technology, one should be aware that an acceptable refinement for the flow problem may not be acceptable for the sensitivity problem.<sup>14</sup>

Figures 4–7 show some of the pitch-rate flow sensitivities results for the case of a NACA 0012 airfoil at several different Mach numbers and at  $\alpha = 0.0$  deg. The calculations were performed around  $q = 0$ , so that the flow solutions required to calculate the source term  $W_B$  and the Jacobians of  $F$  and  $H$  in the sensitivity equation were simply extracted from the Class Code. This implies that for the required flow solutions a standard (inertial) CFD formulation can be used. The origin of coordinates of the body-fixed reference frame was chosen to be at the leading edge.

In Fig. 4 the pitch-rate pressure sensitivity contours and the velocity sensitivity streamlines are shown for a NACA 0012 airfoil at  $M = 0.1$ ; these flow sensitivities were computed using the flow solution shown in Fig. 1. The pressure sensitivities measure how the pressure is going to vary if the airfoil tends to rotate nose up (positive  $q$ ). Similarly, the velocity sensitivities indicate how the velocities are going to change if the airfoil tends to move nose up. Observe that for a positive  $q$  the pressure tends to decrease on the airfoil's upper surface while it tends to increase on the lower surface. From this we expect a positive (upward)  $C_{lq}$ . From the velocity sensitivities streamlines, we see that near the upper surface the flow tends to accelerate while in the lower surface tends to decelerate; also the stagnation point tends to move to the lower surface.

In Fig. 5, a zoom-out of the sensitivity field is shown to display the pressure sensitivity and velocity sensitivity streamlines in the

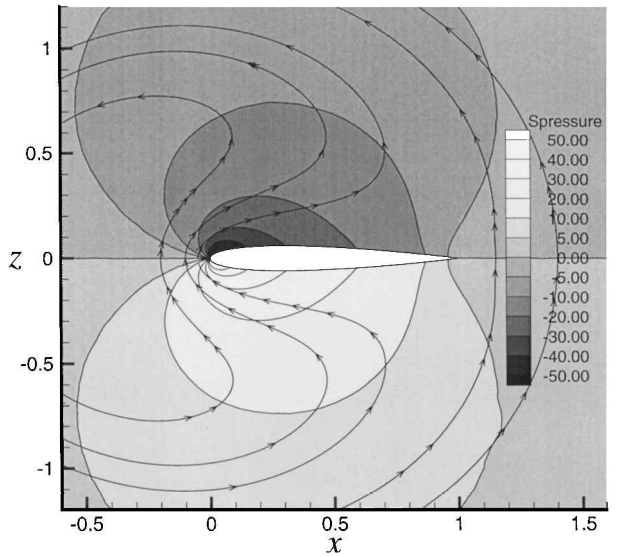


Fig. 4 Pitch-rate pressure sensitivity contours and velocity sensitivity streamlines for a NACA 0012 airfoil at  $M = 0.1$  and  $\alpha = 0.0$  deg.

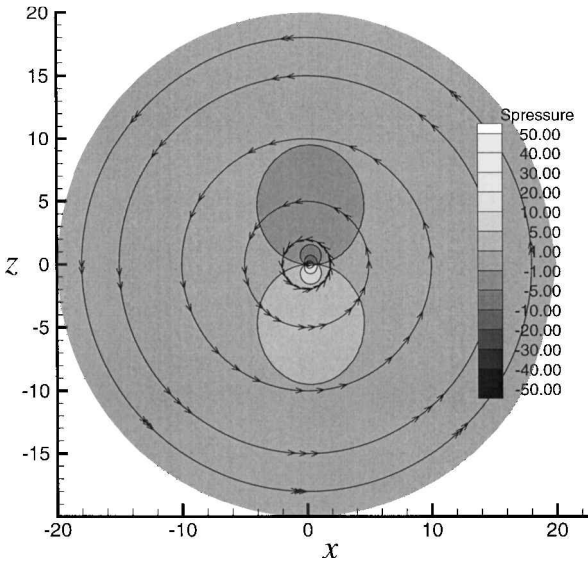


Fig. 5 Pitch-rate pressure sensitivity contours and velocity sensitivity streamlines for a NACA 0012 airfoil at  $M = 0.1$  and  $\alpha = 0.0$  deg (wide view).

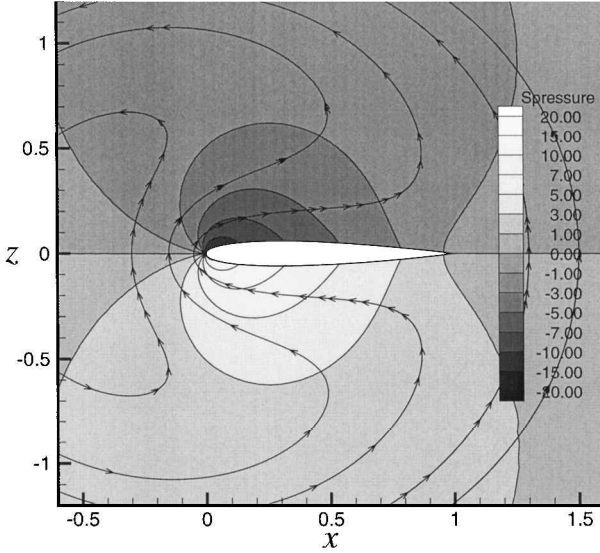


Fig. 6 Pitch-rate pressure sensitivity contours and velocity sensitivity streamlines for a NACA 0012 airfoil at  $M = 0.5$  and  $\alpha = 0.0$  deg.

far field. Observe that the pressure sensitivity goes to zero at the far field. This is expected because airfoil pitch motions should not change the air pressure in the far field. Also observe that the sensitivity streamlines tend to be concentric circles with center at the origin of coordinates, that is, at the airfoil's leading edge. This phenomenon is also expected and can be proved mathematically by differentiating the boundary conditions (11) with respect to  $q$ . Observe that for a positive pitch  $q$ , that is, a pitch in the clockwise sense the far-field sensitivity streamlines run counterclockwise. Note that the finite volume sensitivity formulation allows one to treat the range of subsonic, supersonic, and transonic speeds. In Figs. 6 and 7 the pitch-rate pressure sensitivity and the pitch-rate velocity sensitivity streamlines of the same airfoil are shown but at the higher Mach numbers  $M = 0.5$  and  $0.8$ , respectively. The main features of the resulting pressure sensitivity and velocity sensitivity streamlines for the case  $M = 0.5$  are similar to the low subsonic case.

The case  $M = 0.8$  corresponds to a transonic flow. In particular, as shown in Fig. 2, at  $\alpha = 0.0$  deg, a shock exists on both the upper and lower surfaces of the airfoil, and by symmetry the shocks are located at the same location along the chord. From the corresponding pressure sensitivity shown in Fig. 7, it can be seen that on the upper

Table 1 Computed pitch-rate derivatives

| Coefficient | NISFLOW | QUADPAN | VORLAX |
|-------------|---------|---------|--------|
| $M = 0.1$   |         |         |        |
| $C_{l_q}$   | 10.337  | 10.097  | 9.425  |
| $C_{m_q}$   | -3.489  | -3.424  | -3.151 |
| $M = 0.5$   |         |         |        |
| $C_{l_q}$   | 11.847  | 11.314  | 10.792 |
| $C_{m_q}$   | -3.968  | -3.825  | -3.611 |
| $M = 0.8$   |         |         |        |
| $C_{l_q}$   | 21.889  | 15.713  | 15.408 |
| $C_{m_q}$   | -8.884  | -5.333  | -5.167 |

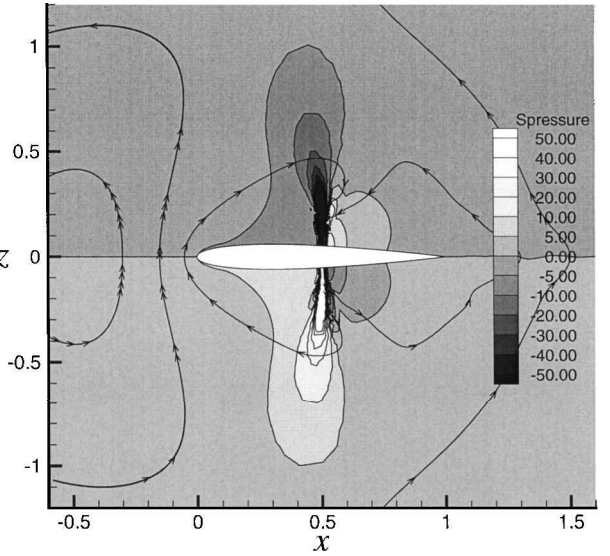


Fig. 7 Pitch-rate pressure sensitivity contours and velocity sensitivity streamlines for a NACA 0012 airfoil at  $M = 0.8$  and  $\alpha = 0.0$  deg.

surface, between the leading edge and some distance before the shock location, the expected change in pressure is a more or less uniform pressure drop. On the lower surface, the expected change is a more or less uniform pressure increase. On the other hand, on the upper surface, near the shock location the expected change is a large pressure drop. This is an indication that the shock moves toward the trailing edge. The opposite phenomenon occurs on the lower surface where the pressure sensitivity is large and positive. This means that the lower-surface shock moves toward the leading edge. Note that the antisymmetry observed in the pressure sensitivity contours with respect to the  $x$  axis is a special phenomenon that only occurs at  $\alpha = 0.0$  deg due to the symmetry of the airfoil and the symmetry of the flow solution at that angle of attack.

Table 1 shows a comparison of the nondimensional pitch-rate derivatives  $C_{l_q} = \partial C_l / \partial \hat{q}$  and  $C_{m_q} = \partial C_m / \partial \hat{q}$  obtained for the three different Mach numbers,  $M = 0.1$ ,  $0.5$ , and  $0.8$ , at  $\alpha = 0.0$  deg. The nondimensional pitch rate  $\hat{q}$  is defined to be  $\hat{q} = q\bar{c}/2V_c$  and, for example, the pitch-damping parameter  $C_{m_q}$  is computed by nondimensionalizing the pitch moment sensitivity [Eq. (27)] in the usual way. To validate the results, Table 1 also shows the same aerodynamic derivatives calculated using QUADPAN<sup>15,16</sup> and VORLAX,<sup>17</sup> which are panel methods and were developed at Lockheed. Both methods are based on potential flow formulations to estimate the local velocity, and they recover the pressure from approximations to the isentropic, compressible Bernoulli equation.

The results show good agreement between QUADPAN and NISFLOW at  $M = 0.1$  and  $0.5$ . The difference in  $C_{l_q}$  is around 2–3% at  $M = 0.1$  and increases to 4–5% at  $M = 0.5$ . For  $C_{m_q}$  the difference is less than 2% at  $M = 0.1$  and increases slightly to less than 4% at  $M = 0.5$ . This small difference may be due to inaccuracies of the discretization and/or to the different approaches used in simulating the pitching motion effect. The estimates at  $M = 0.8$  are quite different. One explanation is that VORLAX and QUADPAN cannot

model embedded shocks, whereas it is clear from the flow solution (see Fig. 2) that at  $M = 0.8$  there is an embedded shock. In addition, the NISFLOW results shown in Table 1 have been validated by comparisons to finite difference estimates based on the nonlinear flow solutions. In subsonic cases, the finite difference estimates are with 0.5% of the NISFLOW values. For the  $M = 0.8$ , the comparison degrades to about 3%, but some of this may be explained by insufficient grid refinement in solving the linear sensitivity equation and/or the nonlinear flow equation.

The comparisons with VORLAX,<sup>17</sup> also shown in Table 1, are somewhat worse. At the lower Mach numbers, the VORLAX values are around 6%/9% smaller in magnitude than those obtained using QUADPAN/NISFLOW. Actually, we expect that the values generated by VORLAX to be less accurate because VORLAX implements a lifting surface panel method, that is, it is based on the approximation that the airfoil has zero thickness.

Observe that the negative values of  $C_{m_q}$  indicates that the moment produced is always in the opposite direction of the pitch rotation, that is, damping in pitch. It also follows from the results that both  $C_{l_q}$  and  $C_{m_q}$  tend to increase in magnitude when the Mach number increases.

## Conclusions

A mathematical model for compressible flow about an aircraft in generalized steady motion has been developed. This required an extension of standard CFD methods to noninertial reference frames. A sensitivity equation method applied to this formulation provides a way to compute rotary stability derivatives. The method was numerically implemented for the case of planar, two-dimensional motions, and the pitch-rate derivatives  $C_{l_q}$  and  $C_{m_q}$  were computed for a NACA 0012 airfoil. The sensitivity-equation method is potentially superior to the panel methods because it is valid for all ranges of Mach numbers, including transonic flow. Also, because it is based on the conservative form of Euler equations, it is more exact than approximations based on the linearized potential flow equations. The method can be extended to the three-dimensional case and to the Reynolds averaged Navier-Stokes equations. The main virtue of the sensitivity-equation approach is that all rotary derivatives can be estimated based on a single solution for the nonlinear fluid mechanics along with three linear sensitivity solutions.

## Acknowledgments

This research was supported, in part, by the Air Force Office of Scientific Research under Grant F49620-96-1-0329 and, in part, by the Air Force Research Laboratory under Contract F33615-98-C-3003. Thanks are extended to R. M. Coopersmith of Lockheed-

California for providing the rate derivatives from QUADPAN and VORLAX and to W. K. Anderson of NASA Langley Research Center for providing his Class Code.

## References

- <sup>1</sup>McRuer, D., Ashkenas, I., and Graham, D., *Aircraft Dynamics and Automatic Control*, Princeton Univ. Press, Princeton, NJ, 1973, pp. 21, 22.
- <sup>2</sup>Tobak, M., and Schiff, L. B., "Aerodynamic Mathematical Modelling—Basic Concepts," *Dynamic Stability Parameters*, AGARD, Lecture Series 114, March 1981 (Lecture 1).
- <sup>3</sup>Godfrey, A. G., and Cliff, E. M., "Direct Calculation of Aerodynamic Force Derivatives: A Sensitivity-Equation Approach," AIAA Paper 98-0393, Jan. 1998.
- <sup>4</sup>Godfrey, A. G., Eppard, W. M., and Cliff, E. M., "Using Sensitivity Equations for Chemically Reacting Flows," AIAA Paper 98-4805, Sept. 1998.
- <sup>5</sup>von Kármán, T., and Burgers, J. M., "General Aerodynamic Theory—Perfect Fluids," *Aerodynamic Theory—A General Review of Progress*, edited by W. F. Durand, California Inst. of Technology, Pasadena, CA, 1943 (originally published in 1934), pp. 230–310.
- <sup>6</sup>Theodorsen, T., "A General Theory of Aerodynamic Instability and the Mechanism of Flutter," NACA Rept. 496, 1935.
- <sup>7</sup>Jones, R. T., "The Unsteady Lift of a Wing of Finite Aspect Ratio," NACA Rept. 681, 1940.
- <sup>8</sup>Herdman, T. L., and Turi, J., "A Natural State-Space Model for an Aerelastic Control System," *Journal of Integral Equations*, Vol. 7, No. 4, 1995, pp. 413–424.
- <sup>9</sup>Mracek, C. P., and Mook, D. T., "Numerical Simulation of Three-Dimensional Lifting Flows by a Vortex Panel Method," AIAA Paper 88-4336-CP, Aug. 1988.
- <sup>10</sup>Etkin, B., *Dynamics of Atmospheric Flight*, Wiley, New York, 1972, Chaps. 4, 5.
- <sup>11</sup>Miele, A., *Flight Performance*, Addison-Wesley, Reading, MA, 1962, Chap. 1.
- <sup>12</sup>Hirsch, C., *Numerical Computation of Internal and External Flows*, Vol. 1, Wiley, New York, 1988, Chap. 1.
- <sup>13</sup>von Mises, R., *Theory of Flight*, Dover, New York, 1959, pp. 570, 571.
- <sup>14</sup>Borggaard, J., and Pelletier, D., "Optimal Shape Design in Forced Convection Using Adaptive Finite Elements," AIAA Paper 98-0908, Jan. 1998.
- <sup>15</sup>Youngren, H. H., Bouchard, E. E., Coopersmith, R. M., and Miranda, L. R., "Comparison of Panel Method Formulations and its Influence on the Development of QUADPAN, an Advanced Low Order Method," AIAA Paper 83-1827, July 1983.
- <sup>16</sup>Johnston, C. E., Youngren, H. H., and Sikora, J. S., "Engineering Applications of an Advanced Low-Order Panel Method," Society of Automotive Engineers, TP Ser. 851793, Oct. 1985.
- <sup>17</sup>Miranda, L. R., Elliott, R. D., and Baker, W. M., "A Generalized Vortex Lattice Method for Subsonic and Supersonic Flow Applications," NASA CR 2865, Dec. 1977.